

PATTERN SYNTHESIS OF CONCENTRIC CIRCULAR ANTENNA ARRAY BY NONLINEAR LEAST-SQUARE METHOD

Hua Guo^{*}, Chenjiang Guo, Yan Qu, and Jun Ding

School of Electronics and Information, Northwestern Polytechnical University, Xi'an 710129, China

Abstract—An improved nonlinear least-square method is presented in this paper. This method changes the traditional least-square method's shortness of being sensitive to its initial conditions. Pattern synthesis for concentric circular arrays using nonlinear least-square method is introduced. The excitation amplitudes and phases of the array elements are optimized. This method can make the design of the feeding network much easier because the excitation amplitudes of the elements placed on the same ring are equal. The number of parameters to be optimized is reduced which leads to a faster simulation speed and makes the simulation results much more accurate. Also, the cost of designing the feeding network is reduced. The simulation results show the good agreement between the synthesized and desired radiation pattern. Also, the peak side lobe level (PSLL) of the synthesized radiation pattern is quite low.

1. INTRODUCTION

Pattern synthesis of array antenna can be seen as a general optimization problem where the excitation amplitudes and phases of array elements are optimized. There are a wide variety of techniques that have been developed for the synthesis of linear and planar arrays [1–21]. To complete this kind of optimization, global optimization methods are usually used, such as genetic algorithms (GA) [3–5], particle swarm optimization (PSO) [6, 7] and differential evolution (DE) algorithm. A hybrid genetic algorithm is used to synthesize desired far-field radiation patterns of conformal antenna array [3]. A comparison study between phase-only and amplitude-phase synthesis of symmetric dual-pattern linear antenna arrays

Received 3 March 2013, Accepted 8 April 2013, Scheduled 13 April 2013

* Corresponding author: Hua Guo (xdguohua@163.com).

using floating-point or real-valued genetic algorithms is given in [4]. Unequally spaced linear array synthesis with side lobe suppression under constraints to beam width and null control using a design technique based on a comprehensive learning particle swarm optimizer (CLPSO) is presented in [6]. Differential evolution algorithm is used in the synthesis of antenna arrays in [8–10]. Planar antenna arrays have much more elements and the radiation patterns are more complex. So, the global optimization methods are hard to use in the synthesis of planar antenna arrays. However, a great deal of research has been done on the synthesis of planar antenna arrays using global optimization method. Planar, sparse and aperiodic arrays are synthesized using an enhanced genetic algorithm in [11]. An optimization method based on an adaptive genetic algorithm has been applied to the real-time control of planar antenna arrays in [12]. The chaotic binary particle swarm optimization (CBPSO) algorithm is presented as a useful alternative for the synthesis of thinned arrays in [13]. But the global optimization methods are usually time consuming. So, many other methods have been used in the pattern synthesis of array antenna [14–19]. Keizer [17] presents a method to synthesize planar arrays with elements in a periodic grid by successively applying the fast Fourier transform (FFT). Projection matrix algorithm (PMA) is applied to fulfill shaped beam synthesis in arrays and reflectors [18]. A synthesis of unequally spaced antenna arrays using Legendre functions is proposed in [19]. These methods are iterative and have the advantage of being fast.

A concentric circular array has the advantage of being compact and provides a rotation of main beam by the shift of the array element excitations [20, 21]. However, if the number of array elements is large, global optimization methods will take a great deal of time to get a satisfied result. For the array elements are not placed in rectangular grids, FFT will be hard applied to the synthesis of this kind of array.

A concentric circular array is a non-uniform planar array and there is no symmetry in its geometry, which will increase the difficulty in the synthesis of this kind of array especially when the desired radiation pattern is complex. Nonlinear least-square method is an iterative method and there is no special requirement for the positions of array elements. Also, with some minor modifications in equations, this method can reduce the optimization complexity and the cost of designing the feeding network greatly. So, an improved nonlinear least-square method is used in the synthesis of concentric circular array. The desired radiation pattern is given and the excitation amplitudes and phases are optimized. Also, two kinds of arrays are considered. One is that all the excitation amplitudes of the elements are optimized and

the other one is only the amplitudes of the elements placed on different rings are optimized. In the second method, the excitation amplitudes of the elements placed on the same ring are equal.

2. OPTIMIZATION MODEL OF ANTENNA ARRAY

Figure 1 shows the general structure of circular array antenna. An array element is disposed at the origin point and the other elements are disposed on some concentric circular rings. Assuming that all elements are isotropic sources, then the antenna factor of the considered geometry is reported in the following relation [21]

$$AF(\theta, \phi) = \sum_{i=1}^R \sum_{l=1}^{N_i} I_{il} \exp(j\alpha_{il}) \exp(jk\rho_i \sin \theta \cos(\phi - \varphi_{il})) \quad (1)$$

where $k = 2\pi/\lambda$ is wave number, λ is wavelength, $\theta \in [0, \pi/2]$ is elevation angle, $\phi \in [0, 2\pi]$ is azimuth angle. R is the number of concentric rings, N_i is the element number of the i th concentric ring, ρ_i is the radius of the i th concentric ring, I_{il} , α_{il} and φ_{il} are the excitation amplitude, excitation phase and azimuth angle of the l th element on i th concentric ring, respectively.

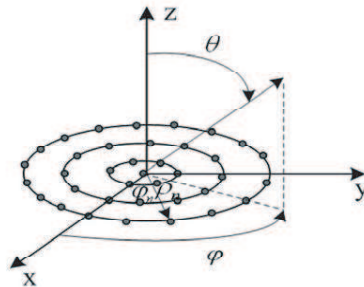


Figure 1. Structure of a concentric circular array.

Assuming that the spacing between the adjacent rings is d_1 , then the radius of i th concentric ring can be determined as

$$\rho_i = (i - 1)d_1, \quad i = 1, 2, \dots, R \quad (2)$$

If the adjacent elements spacing on each concentric ring is greater than or equal to d_2 , then the maximum element number of each ring can be written as

$$N_i = \text{floor} \left(\frac{2\pi\rho_i}{d_2} \right), \quad i = 1, 2, \dots, R \quad (3)$$

where $\text{floor}()$ is rounded down function.

Assuming that the array elements on every concentric ring are uniformly disposed, the azimuth angle of each element can be given by

$$\varphi_{il} = \frac{2\pi\rho_i}{N_i}(l-1), \quad l = 1, 2, \dots, N_i \quad (4)$$

where the azimuth angle of the first element on each concentric ring is zero, then, the azimuth angles of the elements are increased along ϕ direction.

In order to facilitate the application of nonlinear least-square method, each array element is numbered. The number of the element placed at the origin point is 1. The number is increased along the radius of the concentric rings, and the first element on each ring is firstly numbered. Then, (1) can be updated with the following equation

$$AF(\theta, \phi, \xi) = \sum_{n=1}^N I_n \exp(j\alpha_n) \exp(jk\rho_n \sin\theta \cos(\phi - \varphi_n)) \quad (5)$$

where N is the total number of elements, and I_n , α_n , ρ_n and φ_n are the excitation amplitude, excitation phase, radius and azimuth angle of the n th element, respectively. $\xi = [I_1, I_2, \dots, I_N, \alpha_1, \alpha_2, \dots, \alpha_N]$ is the vector of the excitation amplitudes and phases. Taking the excitation amplitudes and phases as the optimization parameters, the total number of the optimization parameters is $2N$.

Assuming $s(\theta, \phi, \xi) = AF((\theta, \phi, \xi))/AF_{\max}$, where AF_{\max} is the maximum value of $AF(\theta, \phi, \xi)$, $s(\theta, \phi, \xi)$ is the normalized pattern function. θ and ϕ are divided into M_1 and M_2 equal parts, respectively. Then, the total discrete points of angle are $M = M_1 \times M_2$. So, the angle of each discrete point is given by

$$\theta_{m_1} = \frac{m_1 - 1}{M_1 - 1} \cdot \frac{\pi}{2}, \quad m_1 = 1, 2, \dots, M_1 \quad (6)$$

$$\phi_{m_2} = \frac{m_2 - 1}{M_2 - 1} \cdot 2\pi, \quad m_2 = 1, 2, \dots, M_2 \quad (7)$$

Let $f(\theta, \phi)$ represents the normalized desired pattern function which is nothing to do with ϕ . The objective function of nonlinear least-square method can be given by

$$r_j(\xi) = \| \|s(\theta_{m_1}, \phi_{m_2}, \xi) - f(\theta_{m_1}, \phi_{m_2})\| \|, \quad j = 1, 2, \dots, M \quad (8)$$

where

$$\| \|s(\theta_{m_1}, \phi_{m_2}, \xi)\| \| = \frac{\sqrt{\left(\sum_{n=1}^N a_n\right)^2 + \left(\sum_{n=1}^N b_n\right)^2}}{AF_{\max}} \quad (9)$$

where

$$a_n = I_n \cos(k\rho_n \sin \theta_{m_1} \cos(\phi_{m_2} - \varphi_n) + \alpha_n) \tag{10}$$

$$b_n = I_n \sin(k\rho_n \sin \theta_{m_1} \cos(\phi_{m_2} - \varphi_n) + \alpha_n) \tag{11}$$

Considering the constraints of excitation amplitudes and phases, the mathematical model of nonlinear least-square method can be expressed as

$$\begin{cases} \min \left(\sum_{j=1}^M r_j(\xi) \right) \\ s.t. 0 \leq \alpha_i \leq 2\pi, \quad 0 \leq I_i \leq 1 \\ i = 1, 2, \dots, N \end{cases} \tag{12}$$

3. OPTIMIZATION STEPS

In order to overcome the impact of matrix singular on the computing precision, Levenbert-Marquardt method is used to calculate the model of nonlinear least-square method. The algorithm steps are given as follows:

Step1. Choose $\xi^{(0)}$ as the initial value, let $\xi_{best} = \xi^{(0)}$, where ξ_{best} is the best solution of optimization parameters, set $r_{best} = (r_j(\xi^{(0)}))^T r_j(\xi^{(0)})$, where r_{best} is the minimum optimization error, give m_{max} and k_{max} , let $m = 0$.

Step2. Give $\beta \in (0, 1)$, $\mu_k > 1$, $\nu > 1$ and $\varepsilon > 0$, $\varepsilon_0 > 0$, $0 < \Delta\varepsilon < 1$, let $k = 0$.

Step3. For $j = 1, 2, \dots, M$, calculate $r_j(\xi^{(k)})$ and $S(\xi^{(k)}) = (r_j(\xi^{(k)}))^T r_j(\xi^{(k)})$.

Step4. For $i = 1, 2, \dots, N$, $j = 1, 2, \dots, M$, calculate $\nabla r_j(\xi^{(k)})$, where $\nabla r_j(\xi^{(k)}) = [J_{ij}(\xi^{(k)})]$, $J_{ij}(\xi^{(k)}) = \frac{\partial r_j(\xi^{(k)})}{\partial \xi_i^{(k)}}$.

If $\|s(\theta_{m_1}, \phi_{m_2}, \xi^{(k)})\| - f(\theta_{m_1}, \phi_{m_2}) \geq 0$, then

$$\begin{aligned} \frac{\partial r_j(\xi^{(k)})}{\partial \alpha_i^{(k)}} &= \frac{\partial \|s(\theta_{m_1}, \phi_{m_2}, \xi^{(k)})\|}{\partial \alpha_i^{(k)}} \\ &= \frac{1}{AF_{max}} \left(\frac{-\sum_{n=1}^N a_n I_i \sin(k\rho_i \sin \theta_{m_1} \cos(\phi_{m_2} - \varphi_i) + \alpha_i)}{\sqrt{\left(\sum_{n=1}^N a_n\right)^2 + \left(\sum_{n=1}^N b_n\right)^2}} \right) \end{aligned}$$

$$\left. + \frac{\sum_{n=1}^N b_n I_i \cos(k\rho_i \sin \theta_{m_1} \cos(\phi_{m_2} - \varphi_i) + \alpha_i)}{\sqrt{\left(\sum_{n=1}^N a_n\right)^2 + \left(\sum_{n=1}^N b_n\right)^2}} \right) \quad (13)$$

$$\begin{aligned} \frac{\partial r_j(\xi^{(k)})}{\partial I_i^{(k)}} &= \frac{\partial \|s(\theta_{m_1}, \phi_{m_2}, \xi^{(k)})\|}{\partial I_i^{(k)}} \\ &= \frac{1}{AF_{\max}} \left(\frac{\sum_{n=1}^N a_n \cos(k\rho_i \sin \theta_{m_1} \cos(\phi_{m_2} - \varphi_i) + \alpha_i)}{\sqrt{\left(\sum_{n=1}^N a_n\right)^2 + \left(\sum_{n=1}^N b_n\right)^2}} \right. \\ &\quad \left. + \frac{\sum_{n=1}^N b_n \sin(k\rho_i \sin \theta_{m_1} \cos(\phi_{m_2} - \varphi_i) + \alpha_i)}{\sqrt{\left(\sum_{n=1}^N a_n\right)^2 + \left(\sum_{n=1}^N b_n\right)^2}} \right) \quad (14) \end{aligned}$$

If $\|s(\theta_{m_1}, \phi_{m_2}, \xi^{(k)})\| - f(\theta_{m_1}, \phi_{m_2}) < 0$, then

$$\begin{aligned} \frac{\partial r_j(\xi^{(k)})}{\partial \alpha_i^{(k)}} &= \frac{\partial \|s(\theta_{m_1}, \phi_{m_2}, \xi^{(k)})\|}{\partial \alpha_i^{(k)}} \\ &= \frac{1}{AF_{\max}} \left(\frac{\sum_{n=1}^N a_n I_i \sin(k\rho_i \sin \theta_{m_1} \cos(\phi_{m_2} - \varphi_i) + \alpha_i)}{\sqrt{\left(\sum_{n=1}^N a_n\right)^2 + \left(\sum_{n=1}^N b_n\right)^2}} \right. \\ &\quad \left. - \frac{\sum_{n=1}^N b_n I_i \cos(k\rho_i \sin \theta_{m_1} \cos(\phi_{m_2} - \varphi_i) + \alpha_i)}{\sqrt{\left(\sum_{n=1}^N a_n\right)^2 + \left(\sum_{n=1}^N b_n\right)^2}} \right) \quad (15) \end{aligned}$$

$$\frac{\partial r_j(\xi^{(k)})}{\partial I_i^{(k)}} = \frac{\partial \|s(\theta_{m_1}, \phi_{m_2}, \xi^{(k)})\|}{\partial I_i^{(k)}}$$

$$= -\frac{1}{AF_{\max}} \left(\frac{\sum_{n=1}^N a_n \cos(k\rho_i \sin \theta_{m_1} \cos(\phi_{m_2} - \varphi_i) + \alpha_i)}{\sqrt{\left(\sum_{n=1}^N a_n\right)^2 + \left(\sum_{n=1}^N b_n\right)^2}} + \frac{\sum_{n=1}^N b_n \sin(k\rho_i \sin \theta_{m_1} \cos(\phi_{m_2} - \varphi_i) + \alpha_i)}{\sqrt{\left(\sum_{n=1}^N a_n\right)^2 + \left(\sum_{n=1}^N b_n\right)^2}} \right) \quad (16)$$

Step5. Calculate $\nabla S(\xi^{(k)}) = (\nabla r_j(\xi^{(k)}))^T r_j(\xi^{(k)})$.

Step6. Let $\mathbf{Q} = (\nabla r_j(\xi^{(k)}))^T \nabla r_j(\xi^{(k)})$, solve equation $[\mathbf{Q} + \mu_k \mathbf{I}]d^{(k)} = -\nabla S(\xi^{(k)})$, where \mathbf{I} represents the unit diagonal matrix.

Step7. Set $\xi^{(k+1)} = \xi^{(k)} + \mathbf{d}^{(k)}$, if $\max(\mathbf{d}^{(k)}) < \varepsilon$ or $k > k_{\max}$, go to step10, otherwise, go to step8.

Step8. If $S(\xi^{(k)}) < S(\xi^{(k)}) + \beta(\nabla S(\xi^{(k)}))^T \mathbf{d}^{(k)}$, set $\mu_k = \mu_k/\nu$, go to step9, otherwise set $\mu_k = \mu_k \times \nu$, go to step6.

Step9. Let $k = k + 1$, go to step3.

Step10. If $S(\xi^{(k+1)}) < \varepsilon_0$ or $m > m_{\max}$, $\xi_{best} = \xi^{(k+1)}$, terminate iteration, otherwise, if $S(\xi^{(k+1)}) < r_{best}$, set $\xi_{best} = \xi^{(k+1)}$, $\xi^{(0)} = \xi^{(0)} + \Delta\varepsilon \times \xi^{(0)} \times \text{rand}(0, 1)$, where $\text{rand}(0, 1)$ is uniformly distributed random numbers between $[0, 1]$, normalize the excitation amplitudes, let $m = m + 1$, go to step2.

Among the above steps, another layer of iteration is added to the traditional nonlinear least-square method. If the solution does not meet the requirements, another vector nearer the former initial value is selected as the initial value and the computation is repeated. The best solution of all the iteration is saved as the ultimate result. This improves the traditional nonlinear least-square method's shortness of dependence on the initial value and increases the optimization ability of nonlinear least-square method.

4. IMPROVED OPTIMIZATION MODEL OF ANTENNA ARRAY

In order to reduce the design difficulty of feeding network, another synthesis method is introduced in this paper. The excitation amplitudes of the elements disposed on the same ring are equal. The far-field radiation pattern of a concentric circular array can be written

as

$$AF(\theta, \phi) = I_1 \exp(j\alpha_1) \exp(jk\rho_1 \sin \theta \cos(\phi - \varphi_1)) + \sum_{i=2}^R \sum_{l=N_{p_i}+1}^{N_{p_{i+1}}} I_i \exp(j\alpha_l) \exp(jk\rho_l \sin \theta \cos(\phi - \varphi_l)) \quad (17)$$

where, $N_{p_i} = \sum_{k=1}^{i-1} N_k$, $i = 2, 3, \dots, R$ represents the element numbers before the i th concentric circle ring. I_i , $i = 1, 2, \dots, R$ is the excitation amplitude of the elements disposed on the i th concentric circle ring. ρ_l , φ_l and α_l , $l = 1, 2, \dots, N$ are the radius, azimuth angle and excitation phase of the l th element. The phase differential has the similar configuration as (13) and (15). The differential of the excitation amplitudes can be updated as follows.

If $\|s(\theta_{m_1}, \phi_{m_2}, \xi^{(k)})\| - f(\theta_{m_1}, \phi_{m_2}) \geq 0$, then

$$\begin{aligned} \frac{\partial r_j(\xi^{(k)})}{\partial I_1^{(k)}} &= \frac{\partial \|s(\theta_{m_1}, \phi_{m_2}, \xi^{(k)})\|}{\partial I_1^{(k)}} \\ &= \frac{1}{AF_{\max}} \left(\frac{\sum_{n=1}^N a_n \cos(k\rho_1 \sin \theta_{m_1} \cos(\phi_{m_2} - \varphi_1) + \alpha_1)}{\sqrt{\left(\sum_{n=1}^N a_n\right)^2 + \left(\sum_{n=1}^N b_n\right)^2}} \right. \\ &\quad \left. + \frac{\sum_{n=1}^N b_n \sin(k\rho_1 \sin \theta_{m_1} \cos(\phi_{m_2} - \varphi_1) + \alpha_1)}{\sqrt{\left(\sum_{n=1}^N a_n\right)^2 + \left(\sum_{n=1}^N b_n\right)^2}} \right) \quad (18) \end{aligned}$$

$$\begin{aligned} \frac{\partial r_j(\xi^{(k)})}{\partial I_i^{(k)}} &= \frac{\partial \|s(\theta_{m_1}, \phi_{m_2}, \xi^{(k)})\|}{\partial I_i^{(k)}} \\ &= \frac{1}{AF_{\max}} \left(\frac{\sum_{n=1}^N a_n \sum_{l=N_{p_i}+1}^{N_{p_{i+1}}} \cos(k\rho_l \sin \theta_{m_1} \cos(\phi_{m_2} - \varphi_l)) + \alpha_l}{\sqrt{\left(\sum_{n=1}^N a_n\right)^2 + \left(\sum_{n=1}^N b_n\right)^2}} \right) \end{aligned}$$

$$\left. \begin{aligned} & + \frac{\sum_{n=1}^N a_n \sum_{l=N_{p_i}+1}^{N_{p_i+1}} \sin(k\rho_l \sin \theta_{m_1} \cos(\phi_{m_2} - \varphi_l)) + \alpha_1}{\sqrt{\left(\sum_{n=1}^N a_n\right)^2 + \left(\sum_{n=1}^N b_n\right)^2}} \end{aligned} \right) \\
 i = 2, 3, \dots, R \quad (19)$$

If $\|s(\theta_{m_1}, \phi_{m_2}, \xi^{(k)})\| - f(\theta_{m_1}, \phi_{m_2}) < 0$, then

$$\begin{aligned} \frac{\partial r_j(\xi^{(k)})}{\partial I_1^{(k)}} &= \frac{\partial \|s(\theta_{m_1}, \phi_{m_2}, \xi^{(k)})\|}{\partial I_1^{(k)}} \\ &= -\frac{1}{AF_{\max}} \left(\frac{\sum_{n=1}^N a_n \cos(k\rho_1 \sin \theta_{m_1} \cos(\phi_{m_2} - \varphi_1)) + \alpha_1}{\sqrt{\left(\sum_{n=1}^N a_n\right)^2 + \left(\sum_{n=1}^N b_n\right)^2}} \right. \\ & \quad \left. + \frac{\sum_{n=1}^N b_n \sin(k\rho_1 \sin \theta_{m_1} \cos(\phi_{m_2} - \varphi_1)) + \alpha_1}{\sqrt{\left(\sum_{n=1}^N a_n\right)^2 + \left(\sum_{n=1}^N b_n\right)^2}} \right) \end{aligned} \quad (20)$$

$$\begin{aligned} \frac{\partial r_j(\xi^{(k)})}{\partial I_i^{(k)}} &= \frac{\partial \|s(\theta_{m_1}, \phi_{m_2}, \xi^{(k)})\|}{\partial I_i^{(k)}} \\ &= -\frac{1}{AF_{\max}} \left(\frac{\sum_{n=1}^N a_n \sum_{l=N_{p_i}+1}^{N_{p_i+1}} \cos(k\rho_l \sin \theta_{m_1} \cos(\phi_{m_2} - \varphi_l)) + \alpha_1}{\sqrt{\left(\sum_{n=1}^N a_n\right)^2 + \left(\sum_{n=1}^N b_n\right)^2}} \right. \\ & \quad \left. + \frac{\sum_{n=1}^N a_n \sum_{l=N_{p_i}+1}^{N_{p_i+1}} \sin(k\rho_l \sin \theta_{m_1} \cos(\phi_{m_2} - \varphi_l)) + \alpha_1}{\sqrt{\left(\sum_{n=1}^N a_n\right)^2 + \left(\sum_{n=1}^N b_n\right)^2}} \right) \\ & \quad i = 2, 3, \dots, R \quad (21) \end{aligned}$$

where a_n and b_n are the real part and imaginary part of (17), which have the similar configuration as (10) and (11).

5. DESIRED RADIATION PATTERN FUNCTION

The desired pencil beam pattern function can be expressed as

$$f(\theta_{m_1}, \phi_{m_2}) = \begin{cases} \cos^{m_H}(\theta_{m_1} - \theta_H), & \theta_H - \theta_h \leq \theta_{m_1} \leq \theta_H + \theta_h \\ 0.01, & \text{else} \end{cases} \quad (22)$$

where, θ_H is the beam scanning angle of array antenna. $2\theta_h$ is the width of main lobe. m_H is a constant that can be determined by

$$m_H = -\frac{2}{\log_{10}(\cos(\theta_h))} \quad (23)$$

6. OPTIMIZATION RESULTS

In this section, several simulation results of different kinds of radiation patterns are presented. The achieved results show the effectiveness and feasibility of the proposed method. We choose the parameters used in those above expressions as follows: $d_1 = d_2 = \lambda/2$, $R = 7$, $N_1 = 1$, $N_2 = 6$, $N_3 = 12$, $N_4 = 18$, $N_5 = 25$, $N_6 = 31$, $N_7 = 37$, $M_1 = 91$, $M_2 = 181$, $\beta = 0.4$, $\mu_k = |r_j(\xi^{(0)})|$, $\nu = 0.2$, $\varepsilon_0 = \varepsilon = 10^{-6}$, $\Delta\varepsilon = 0.02$, $m_{\max} = 60$, $k_{\max} = 200$. The diameter of the concentric circular array antenna is 6λ and the total element number is 130. The number of the discrete points for angle is 16471.

Example 1: As the first example, all the excitation amplitudes and phases of array elements are optimized. The elevation cut of the desired radiation pattern is as shown in Figure 2(b). It is a pencil

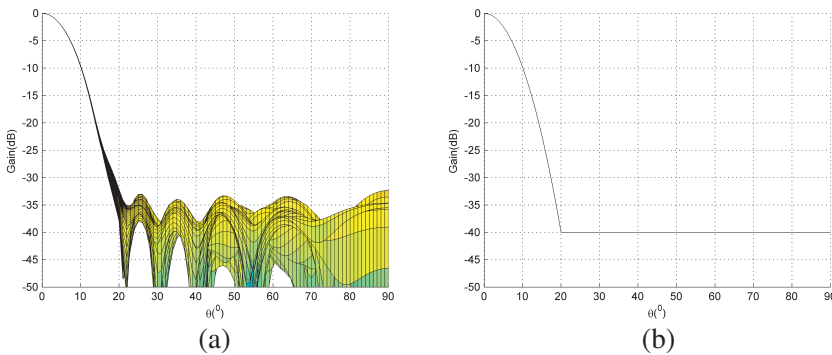


Figure 2. Elevation cut of the radiation pattern for all the excitation are optimized: (a) the synthesized radiation pattern; (b) the desired radiation pattern.

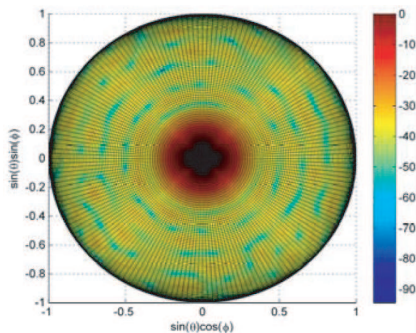


Figure 3. Synthesized radiation pattern for all the excitation amplitudes are optimized.

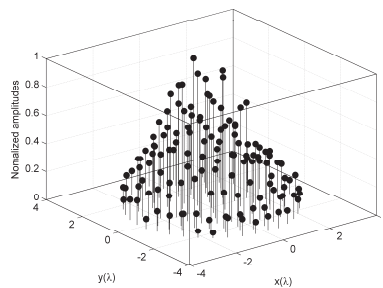


Figure 4. Amplitude distribution for all the excitation amplitudes are optimized.

beam and the radiation pattern does not change along ϕ direction. The beam scanning angle θ_H and the main lobe width $2\theta_h$ in (22) are selected as 0° and 40° , respectively. Then m_H can be determined by (23) as 74. The half-power beam width (HPBW) of the desired radiation pattern is 11.04° . Figure 2(a) shows the elevation cut of the synthesized radiation pattern for all the excitation amplitudes are optimized. From Figure 2(a), we can see that the synthesized pattern has a good agreement with the desired radiation pattern in main lobe area. The PSLL of the synthesized radiation pattern is lower than -30 dB. Figure 3 shows the top view of the synthesized radiation pattern in u - v coordinate where $\mu = \sin\theta \cos\phi$ and $\nu = \sin\theta \sin\phi$. In this example, the number of the parameters to be optimized is 260. Figure 4 gives the amplitude distribution for this example. The amplitudes distribution has a dynamic range ratio (I_{\max}/I_{\min}) of 32.7. The difficulty and cost of designing the feeding network will be increased.

Example2: In example 1, there are too many parameters to be optimized and the dynamic range ratio is too large. To diminish the optimization complexity, the elements on one ring have the same amplitude distribution but vary from one ring to others. In this case, only seven excitation amplitudes are optimized. The desired radiation pattern are chosen as the same as shown in Figure 2(b). Table 1 gives the amplitudes distribution of the elements disposed on each ring. Only seven excitation amplitudes are optimized which will reduce the complexity of optimization. Also, the cost of feeding network is reduced. Figure 5 shows the elevation cut of the synthesized radiation pattern. We can observe from Figure 5 that the PSLL is below -35 dB

and the synthesized result is very similar to the desired result in main lobe area. Figure 6 shows the top view of the radiation pattern in this excitation.

Table 1. Excitation amplitudes distribution for the excitation amplitudes of the elements placed on the same ring are equal.

Ring number	1	2	3	4	5	6	7
Excitation amplitudes	0.8783	1.0000	0.8335	0.2194	0.9062	0.3228	0.1547

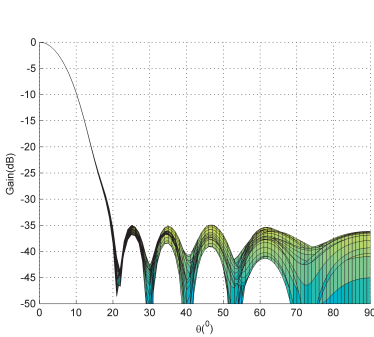


Figure 5. Elevation cut of the radiation pattern for the excitation amplitudes of the elements placed on the same ring are equal.

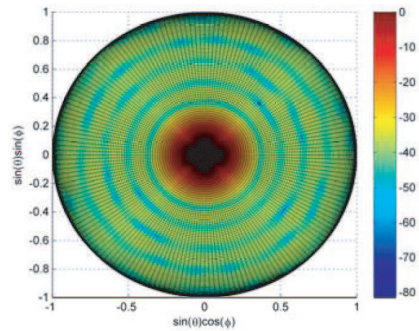


Figure 6. Synthesized radiation pattern for the excitation amplitudes of the elements placed on the same ring are equal.

Example3: In above two examples, the desired radiation pattern is too simple. Many global optimization methods can obtain good synthesis results [2]. In order to show the effectiveness of nonlinear least-square method, a radiation pattern with a nonzero scanning angle is synthesized. We select the beam scanning angle θ_H as 30° . The other parameters are chosen as the same as the above two examples. Table 2 shows the excitation amplitudes of each ring. Figure 7(a) and Figure 7(b) show the elevation cut of the synthesized and desired radiation pattern. From Figure 7(a), we can see that the main lobe width of the synthesized radiation pattern becomes slightly narrower than that of the desired pattern and the PSL is lower than -20 dB. Figure 8 shows the top view of the radiation pattern in this condition. A normal personal computer Intel Core i3 530 @2.93 GHz CPU and 2 GB of RAM is used and the synthesis is programmed using MATLAB

version 7.1. The total synthesis time for one iteration is less than 15 minutes. Because the elements number of antenna array is large and the radiation pattern is complex, it will take more time for global optimization methods to get a satisfied result. Also, in some cases, good result will not be obtained.

Table 2. Excitation amplitude distribution for the scanning angle of 30° .

Ring number	1	2	3	4	5	6	7
Excitation amplitudes	0.0025	0.5800	1.0000	0.2508	0.3411	0.0987	0.1107

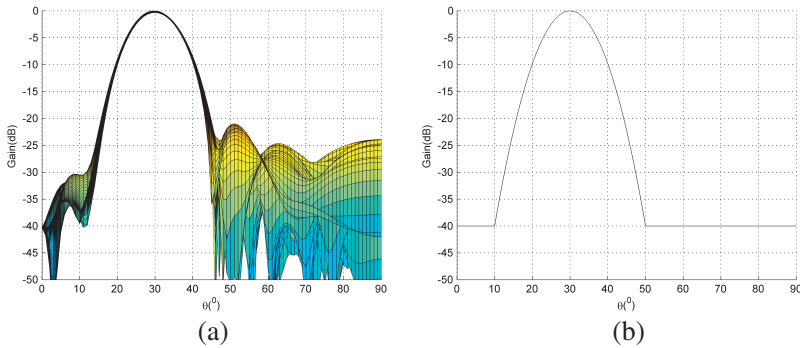


Figure 7. Elevation cut of the radiation pattern for the scanning angle of 30° : (a) the synthesized radiation pattern; (b) the desired radiation pattern.

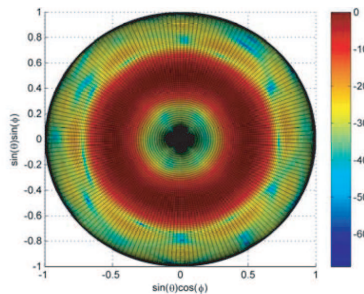


Figure 8. Synthesized radiation pattern for the scanning angle of 30° .

7. CONCLUSION

Nonlinear least-square optimization method is efficiently used in pattern synthesis when the desired pattern is given. A new feeding method is introduced in this paper. The radiation pattern synthesized by this method is very similar to the desired radiation pattern in the main lobe area and has a low PSLL. The PSLL of the synthesized radiation pattern with scanning angle of 0° and 30° is lower than -35 dB and -20 dB, respectively. This method can be extended to other kinds of arrays and other kinds of desired patterns. Also, this method can be used in phase only and amplitude only optimization of antenna arrays. This method can also be used in the synthesis of phase-only reconfigurable arrays.

ACKNOWLEDGMENT

This work was supported by the National Defense Pre-Research Foundation of China under Grant No. 9140A01010412HK03004 and the Aerospace Innovation Fund under Grant No. HTCXJJKT-22.

REFERENCES

1. Yang, K., Z.-Q. Zhao, and Q.-H. Liu, "Fast pencil beam pattern synthesis of large unequally spaced antenna arrays," *IEEE Trans. Antennas and Propag.*, Vol. 61, No. 2, 627–634, 2013.
2. Li, F., Y.-H. Jiao, L.-S. Ren, Y.-Y. Chen, and L. Zhang, "Pattern synthesis of concentric ring array antennas by differential evolution algorithm," *Journal of Electromagnetic Waves and Applications*, Vol. 25, Nos. 2–3, 421–430, 2011.
3. Xu, Z., H. Li, Q.-Z. Liu, and J.-Y. Li, "Pattern synthesis of conformal antenna array by the hybrid genetic algorithm," *Progress In Electromagnetics Research*, Vol. 79, 75–90, 2008.
4. Mahanti, G. K., A. Chakrabarty, and S. Das, "Phase-only and amplitude-phase only synthesis of dual-beam pattern linear antenna arrays using floating-point genetic algorithms," *Progress In Electromagnetics Research*, Vol. 68, 247–259, 2007.
5. Oliveri, G. and A. Massa, "Genetic algorithm (GA)-enhanced almost difference set (ADS)-based approach for array thinning," *IET Microwaves, Antennas & Propagation*, Vol. 5, 305–315, 2011.
6. Goudos, S. K., V. Moysiadou, T. Samaras, K. Siakavara, and J. N. Sahalos, "Application of a comprehensive learning particle swarm optimizer to unequally spaced linear array synthesis with sidelobe level suppression and null control," *IEEE Antennas and Wireless Propagation Letters*, Vol. 9, 125–129, 2010.

7. Zaharis, Z. D. and T. V. Yioultis, "A novel adaptive beamforming technique applied on linear antenna arrays using adaptive mutated Boolean PSO," *Progress In Electromagnetics Research*, Vol. 117, 165–179, 2011.
8. Rocca, P., G. Oliveri, and A. Massa, "Differential evolution as applied to electromagnetics," *IEEE Antennas and Propagation Magazine*, Vol. 53, 38–49, 2011.
9. Mallipeddi, R., J. P. Lie, P. N. Suganthan, S. G. Razul, and C. M. S. See, "A differential evolution approach for robust adaptive beamforming based on joint estimation of look direction and array geometry," *Progress In Electromagnetics Research*, Vol. 119, 381–394, 2011.
10. Li, R., L. Xu, X.-W. Shi, N. Zhang, and Z.-Q. Lv, "Improved differential evolution strategy for antenna array pattern synthesis problems," *Progress In Electromagnetics Research*, Vol. 113, 429–441, 2011.
11. Donelli, M., S. Caorsi, F. De Natale, D. Franceschini, and A. Massa, "A versatile enhanced genetic algorithm for planar array design," *Journal of Electromagnetic Waves and Applications*, Vol. 18, No. 11, 1533–1548, 2004.
12. Massa, A., S. Caorsi, A. Lommi, M. Donelli, and F. De Natale, "Planar antenna array control with genetic algorithms and adaptive array theory," *IEEE Trans. Antennas and Propag.*, Vol. 52, No. 11, 2919–2924, 2004.
13. Wang, W.-B., Q. Feng, and D. Liu, "Synthesis of thinned linear and planar antenna arrays using binary PSO algorithm," *Progress In Electromagnetics Research*, Vol. 127, 371–387, 2012.
14. Qu, Y., G. Liao, S.-Q. Zhu, and X.-Y. Liu, "Pattern synthesis of planar antenna array via convex optimization for airborne forward looking radar," *Progress In Electromagnetics Research*, Vol. 84, 1–10, 2008.
15. Comisso, M. and R. Vescovo, "Fast iterative method of power synthesis for antenna arrays," *IEEE Trans. Antennas and Propag.*, Vol. 57, No. 7, 1952–1962, 2009.
16. Liu, Y., Z.-P. Nie, and Q. H. Liu, "A new method for the synthesis of non-uniform linear arrays with shaped power patterns," *Progress In Electromagnetics Research*, Vol. 107, 349–363, 2010.
17. Keizer, W. P. M. N., "Fast low-sidelobe synthesis for large planar array antennas utilizing successive fast Fourier transforms of array factor," *IEEE Trans. Antennas and Propag.*, Vol. 55, No. 3, 715–722, 2007.

18. Bhattacharyya, A. K., "Projection matrix method for shaped beam synthesis in phased arrays and reflectors," *IEEE Trans. Antennas and Propag.*, Vol. 55, No. 3, 675–683, 2007.
19. Sanchez, J., D. H. Covarrubias-Rosales, and M. A. Panduro, "A synthesis of unequally spaced antenna arrays using Legendre functions," *Progress In Electromagnetics Research M*, Vol. 7, 57–69, 2009.
20. Azevedo, J. A. R., "Synthesis of planar arrays with elements in concentric rings," *IEEE Trans. Antennas and Propag.*, Vol. 59, No. 3, 839–845, 2011.
21. Pathak, N. N., G. K. Mahanti, S. K. Singh, J. K. Mishra, and A. Chakraborty, "Synthesis of thinned planar circular array antennas using modified particle swarm optimization," *Progress In Electromagnetics Research Letters*, Vol. 12, 87–97, 2009.